AIP | Applied Physics Letters

Mechanically tunable terahertz metamaterials

Jining Li, Charan M. Shah, Withawat Withayachumnankul, Benjamin S.-Y. Ung, Arnan Mitchell et al.

Citation: Appl. Phys. Lett. **102**, 121101 (2013); doi: 10.1063/1.4773238
View online: http://dx.doi.org/10.1063/1.4773238
View Table of Contents: http://apl.aip.org/resource/1/APPLAB/v102/i12
Published by the AIP Publishing LLC.

Mechanically tunable terahertz metamaterials

Jining Li,[1,2,a)] Charan M. Shah,[3] Withawat Withayachumnankul,[1] Benjamin S.-Y. Ung,[1] Arnan Mitchell,[3] Sharath Sriram,[3] Madhu Bhaskaran,[3,b)] Shengjiang Chang,[2] and Derek Abbott[1]
[1]*School of Electrical and Electronic Engineering, The University of Adelaide, Adelaide, SA 5005, Australia*
[2]*Institute of Modern Optics, Nankai University, Tianjin 300071, China*
[3]*Functional Materials and Microsystems Research Group, RMIT University, Melbourne, VIC 3001, Australia*

(Received 24 September 2012; accepted 10 December 2012; published online 25 March 2013)

Electromagnetic device design and flexible electronics fabrication are combined to demonstrate mechanically tunable metamaterials operating at terahertz frequencies. Each metamaterial comprises a planar array of resonators on a highly elastic polydimethylsiloxane substrate. The resonance of the metamaterials is controllable through substrate deformation. Applying a stretching force to the substrate changes the inter-cell capacitance and hence the resonance frequency of the resonators. In the experiment, greater than 8% of the tuning range is achieved with good repeatability over several stretching-relaxing cycles. This study promises applications in remote strain sensing and other controllable metamaterial-based devices. © *2013 American Institute of Physics*. [http://dx.doi.org/10.1063/1.4773238]

Metamaterials refer to artificial composites made of dense arrays of sub-wavelength resonators. They allow manipulation of electromagnetic waves in unique ways. Metamaterials containing a wire-grid structure can dilute the electron plasma, changing the plasma frequency, resulting in a negative permittivity at a desired frequency.[1] Metamaterials with split-ring resonators (SRRs) or cut-wire pairs can exhibit a magnetic response with a negative permeability.[2] By combining wire grids and SRRs, negative-index materials can be realized.[3] Based on these controllable electromagnetic properties, metamaterials promise unprecedented opportunities to explore a variety of applications, including superlenses,[4] invisibility cloaks,[5] perfect absorbers,[6] and sensors.[7,8]

Recently, metamaterials scaled to operate at terahertz frequencies have attracted great interest. As opposed to most natural materials, metamaterials can exhibit a strong magnetic or electric response in the terahertz regime. Most metamaterials provide functionality only within a narrow spectral range; however, in many cases, it is desirable to adapt a metamaterial to its environment by tuning its frequency. Numerous tunability approaches have been reported. For example, planar terahertz metamaterials have been tuned by mechanically loading dielectrics or liquids onto their surface[9,10] and also by integrating semiconductors[11] or carbon nanotubes[12] within the structure to provide electronic or optical control of the resonance frequency.

With the advancement of polymer technology and lithographic techniques, it is possible to fabricate metamaterials on thin flexible substrates, including Kapton polyimide,[13,14] polyethylene naphthalate (PEN),[15,16] and polydimethylsiloxane (PDMS).[17] Conformal deformation of flexible terahertz metamaterials has been demonstrated with some reports showing that wrapping these materials onto cylinders with different radii can adjust their resonance frequencies,[18,19] while another reports shows that wrinkling a rigid metamaterial on a soft backing layer surface can influence the response.[20] However, the ability to realize such structures on elastic substrates presents further opportunities for tuning via mechanical stretching and compression. If mechanical stretching is considered as a tuning mechanism, one important consideration is the recoverability of printed structures and their substrates. During operation, the response of metamaterials may potentially be degraded by irreversible physical changes in the metallic elements. Further, the substrate may not be able to fully recover after a certain point or multiple rounds of deformation.

In this letter, we present metamaterials realized on elastic substrates with frequency characteristics that can be tuned by up to 8.3% by mechanical stretching. The structures are designed to fully recover when relaxed and can be repeatedly deformed without degradation. These metamaterials consist of planar arrays of I-shaped resonant elements deposited on a thin PDMS film, which is a flexible polymer with excellent mechanical durability, yet low loss at terahertz frequencies.[17] By utilizing an interdigitated gap structure in the field confinement area of the resonators, a higher Q factor and hence an improved sensitivity can be achieved. The experiments demonstrate the continuous tunability of the structures under an applied uniaxial stretching force. In addition, the robustness of the fabricated metamaterials is validated through repetitive stretching-relaxing cycles.

An I-shaped resonator is chosen to realize metamaterials that are sensitive to mechanical stretching. A modeled array of I1 resonators comprises a thin gold layer, sandwiched between the PDMS substrate layer, and a PDMS encapsulation layer. The thicknesses of the substrate, metal, and the encapsulation layer are modeled as 100 μm, 200 nm, and 10 μm, respectively. Full details of the unit-cell design are further illustrated in Fig. 1(a). To predict the electromagnetic behavior of the resonator, the structure is simulated by using CST MICROWAVE STUDIO. The simulated field at resonance can be found in Fig. 1(b). When the terahertz wave is transmitted

a)Author to whom correspondence should be addressed. Electronic mail: andrewli@eleceng.adelaide.edu.au.
b)E-mail: madhu.bhaskaran@rmit.edu.au.

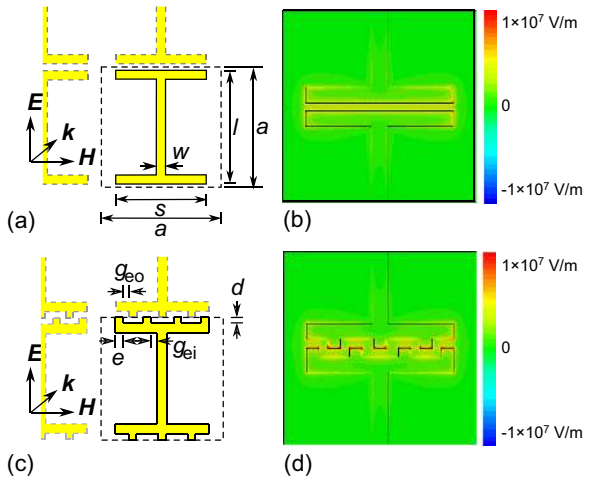

FIG. 1. Metamaterial designs. (a) and (c) Unit cell of designs I1 and I2, respectively. (b) and (d) Electric field distribution at the resonance frequency for designs I1 and I2, respectively. The dimensions of the structures are as follows: $a = 63\,\mu$m, $s = 48\,\mu$m, $l = 60\,\mu$m, $w = 5\,\mu$m, $d = 3\,\mu$m, $e = 4\,\mu$m, $g_{eo} = 3\,\mu$m, and $g_{ei} = 4\,\mu$m. The directions of the propagation and polarization are indicated.

through the metamaterial with the polarization perpendicular to the gaps, the resonators collectively develop a dipole resonance. The resultant dipole resonance frequency can be approximately evaluated from the equivalent inductance and capacitance in the form of $f_0 = 1/(2\pi\sqrt{LC})$. At resonance, the incident electric field induces a large accumulation of surface charges in the metal strips forming the gap, causing a strong electric field in the gap. When a stretching force is applied along the polarization direction, macroscopic deformation results in an expansion in the gap width of the resonators and consequently a reduction in the gap capacitance. By considering that the thickness of the metal layer is much smaller than the width of the metal strips and the gap, the capacitance model of two finite parallel lines on a dielectric plane can be expressed as[21,22]

$$C \approx \epsilon_0 \epsilon_r \left\{ 1.15\left(\frac{2t}{g}\right) + 2.80\left(\frac{2w}{g}\right)^{0.222} \right\} s, \qquad (1)$$

where ϵ_0 is the permittivity of free space, ϵ_r is the relative permittivity of the substrate material, t is the thickness of the metal layer, w is the width of metal strips, $g = a - l$ is the gap width, and s is the length of the metal strips. As the resonance frequency is inversely proportional to the capacitance, the resonance frequency shifts to higher frequencies with increasing gap width.

As an extension to the I1 design, the straight capacitive gap is replaced by an interdigitated gap. In the I2 design, the fingers in the gap are oriented parallel to the intended operating polarization. All dimensions and materials are the same as those in design I1, except for the interdigitated fingers. A diagram of the interdigitated structure and the simulated electric fields at resonance is presented in Figs. 1(c) and 1(d), respectively. The interdigitated gap provides a higher capacitance through a longer effective gap length.[23] An increase in the gap capacitance should lead to a stronger coupling and consequently the Q factor should be greatly enhanced.[24,25]

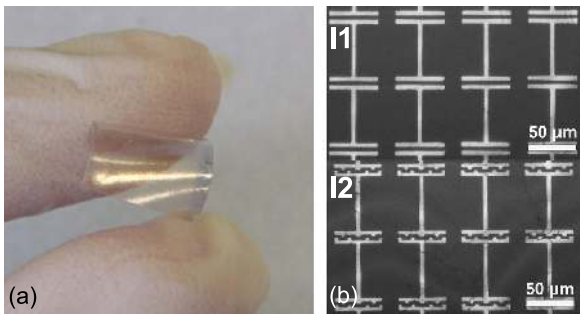

FIG. 2. Fabricated terahertz metamaterials. (a) Photograph of the sample showing its flexibility. (b) Optical micrograph of two fabricated metamaterials.

The resonator structures are fabricated for experimental validation by utilizing standard microfabrication techniques that are adapted to flexible, elastomeric device fabrication.[26] The resonators are made by patterning thin layers of metal film deposited on flexible PDMS substrate. The substrate layer for the resonator structures is obtained by spin coating PDMS on to a silicon wafer[27] to obtain a thickness of 100 μm. Metal layers are deposited on the cured-PDMS coated wafer using electron beam evaporation at room temperature. First, a thin layer of chromium (20 nm) is deposited, to enable adhesion of the gold metal layer, followed by gold (200 nm) deposition on the PDMS substrate. The metal layers are patterned using standard photolithography techniques. The fabrication process is completed by spin coating and curing a final layer of PDMS (10 μm) on top of the above patterned sample. This encapsulates the gold films underneath and avoids any possible damage that could result from the planned stretching experiments. The completed resonator structure is peeled off from the supporting silicon substrate to realize arrays of both I1 and I2 resonator designs as shown in Fig. 2.

The measurement is performed by means of a fiber-coupled terahertz time-domain spectroscopy system (THz-TDS) (Tera K15, Menlo Systems GmbH), as shown in Fig. 3(a). The system bandwidth is approximately 4 THz with a peak dynamic range of 76 dB at 300 GHz. The terahertz wave from the emitter is collimated and focused onto the center of the sample with a beam diameter of approximately 2 mm, covering thousands of the resonators. The fabricated metamaterial is mounted using two plastic clamps on a custom-made test jig, as shown in Fig. 3(b), which allows the stretching of samples with micrometer precision. An aperture with a 12 mm diameter in the metal base of the jig

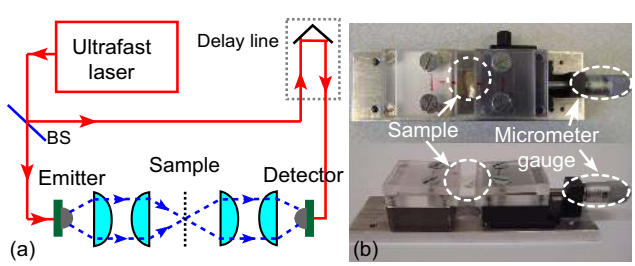

FIG. 3. Experimental setup. (a) A schematic of the employed THz-TDS system. (b) Top and side views of the test jig for stretching metamaterials with controllable strain.

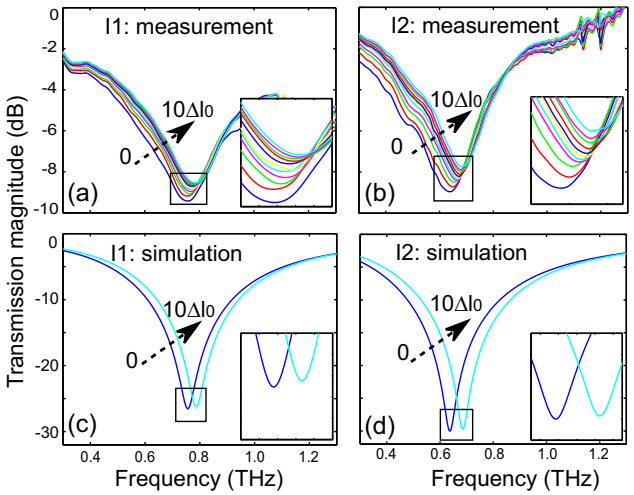

FIG. 4. Transmission magnitude of the I1 design ((a), (c)) and the I2 design ((b), (d)). Plots ((a), (b)) and ((c), (d)) show the experimental and simulation results, respectively. The structures are stretched from 0 to $10\Delta l_0$ with a step size of Δl_0.

allows for transmission-mode measurements. The stretching is applied in discrete steps with $\Delta l_0 = 65\,\mu$m defining the step size, equal to 1% strain of the initial sample length $l_0 = 6.54$ mm and $\Delta l_0 = 65\,\mu$m. During experiments, the strain is varied up to 10%. At each Δl_0 step, the sample is held in a fixed position for 45 min, and during this time the measurements are repeated 3 times.

The terahertz transmission response of I1 is presented in Fig. 4(a). The initial resonance of I1 at its relaxed position is equal to 0.76 THz. When the stretching force is applied, the resonance frequency shifts upwards by approximately 30 GHz to 0.79 THz or about 4% with the strain changing from 0 to $10\Delta l_0$. The I2 structure is also measured by using the same procedure and the measured THz response is presented in Fig. 4(b). It is clear that the initial resonance frequency of I2 is slightly lower than that of I1 due to an increase in the capacitance in the gaps. Under stretching, the resonance frequency shifts from 0.64 THz to 0.68 THz or about 6.3% with the strain changing from 0 to $10\Delta l_0$. Comparing the I2 design in Fig. 4(b) with the I1 design in Fig. 4(a), it is clear that the I2 design has a Q factor of approximately 10% greater and exhibits a higher sensitivity to the applied strain than the I1 design.

When viewing under the microscope, as shown in Fig. 5, both the gap size and the resonator length change by stretching the substrate under 10% strain. The resonator length (l) changes by approximately 1 μm, and the gap size (g) changes by approximately 1.5 μm. As mentioned earlier, a larger gap size causes a blue-shift in the resonance frequency. On the other hand, a longer resonator causes a red-shift. These two effects counteract each other. Since the resonance frequency is more sensitive to the gap size change, the ultimate effect is a blue-shift in the resonance. This can be confirmed by the simulation results in Fig. 4(c), where the gap size is changed from 3 to 4.5 μm or about 50%, and the resonator length is changed from 60 to 61 μm. In the case of design I1, the resonance frequency shifts upwards by 4.2%, and in the case of I2, the resonance frequency shifts by 6.6%. This is close to the measurable 4% and 6.3% shifts in I1 and I2, respectively. A difference in the transmission magnitude between the simulation and experimental results is ascribed to the loss and tolerances in the fabricated metamaterials.

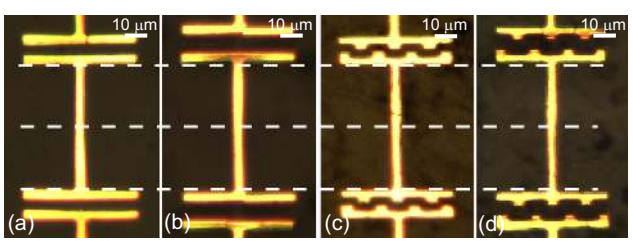

FIG. 5. Optical micrographs of the resonators in the center of samples. (a) and (b) I1 design in relaxed and stretched positions, respectively. (c) and (d) I2 design in relaxed and stretched positions, respectively. The applied strain in (b) and (d) is equal to 10%. The dashed lines are for visual guidance.

To characterize the reversibility and repeatability of the mechanically tunable metamaterials, the process of stretching and releasing is repeated several times. Each metamaterial sample is stretched in 1% strain steps up to 10% and then relaxed in the same discrete steps back to the initial position. As shown in Figs. 6(a) and 6(b) for both structures, the resonance frequency returns to close to the initial value after completing a stretching cycle with only a small hysteresis loop evident. This implies that the resonators and hence the substrate fully recover to the initial position.

Figures 6(b)–6(d) show the measured resonance frequency of structures of type I2 during the 1st, 2nd, and 5th stretching-releasing cycles. The first three cycles have an interval of 24 h between them, and the time delay before the 4th and 5th cycles is increased to more than 48 h. Remarkably, the resonance frequency of the sample without applied strain moves downwards during the priming cycle, from 0.64 THz to approximately 0.60 THz, and then becomes steady in subsequent cycles. This can be attributed to mobility of microcracks in the metallic resonators.[28] Initially, the thin gold layer deposited on the PDMS substrate has a

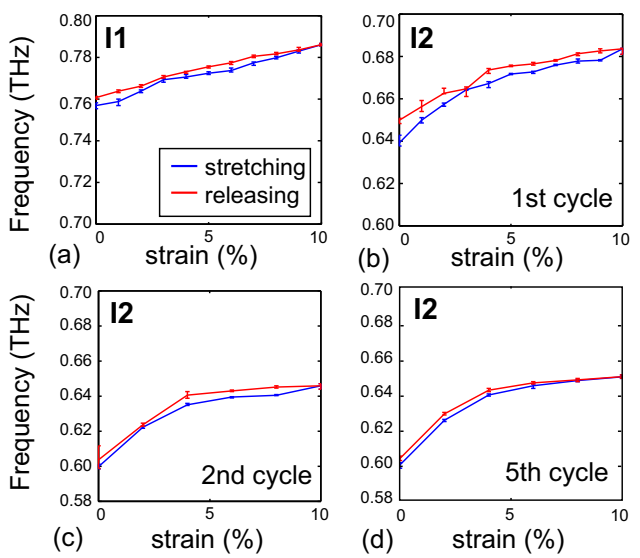

FIG. 6. Resonance frequency as a function of the strain. (a) and (b) First stretching cycle for designs I1 and I2, respectively. (c) and (d) Design I2 in different stretching cycles.

wrinkled structure, and contains surface microcracks within the order of micrometers or less. As reported in the literature on flexible electronics,[26,28] the first stretching cycle serves as a priming cycle. Over the course of this priming cycle, the distribution of gold microcracks attains an equilibrium state between the two PDMS layers enabling repeatable strain performance. As a result, the effective length of each resonator increases slightly, which induces a red-shift in the resonance frequency. Notably, the tunable range is enhanced from 6.3% to 8.3% after the first stretching cycle, as can be observed in Figs. 6(b) and 6(d). This effect results from an improved elasticity of the gold-PDMS substrate.[26] The thin elastomeric substrate and the gold layer with distributed microcracks both become more stable for subsequent stretching cycles, resulting in the reversible stretchability, as evidenced by Figs. 6(c) and 6(d).

In this letter, two types of mechanically tunable planar metamaterials are fabricated and characterized in the terahertz frequency range. Utilizing resonant elements on a highly elastomeric substrate, a continuous tunability of the resonance frequency is achieved with a small applied strain. By adding interdigitated gaps to the resonators, a higher Q factor and larger frequency shift can be obtained. The response of metamaterials is fully recoverable in repeated stretching cycles after an initial priming cycle. This work suggests potential applications of metamaterials in biocompatible strain sensing.

J.L. acknowledges National High Technology Research and Development Program of China (Grant No. 2011AA010205) and National Natural Science Foundation of China (Grant No. 61171027). W.W., S.S., and M.B. acknowledge Australian Post-Doctoral Fellowships from the Australian Research Council (ARC) through Discovery Project Nos. DP1095151, DP110100262, and DP1092717, respectively. D.A. and W.W. also acknowledge funding from ARC Discovery Project No. DP120100200. Technical assistance from Ian Linke, Alban O'Brien, Brandon Pullen, Hungyen Lin, and Tiaoming Niu is appreciated.

[1]J. B. Pendry, A. J. Holden, W. J. Stewart, and I. Youngs, Phys. Rev. Lett. **76**, 4773 (1996).
[2]J. B. Pendry, A. J. Holden, D. J. Robbins, and W. J. Stewart, IEEE Trans. Microwave Theory Tech. **47**, 2075 (1999).
[3]D. R. Smith, W. J. Padilla, D. C. Vier, S. C. Nemat-Nasser, and S. Schultz, Phys. Rev. Lett. **84**, 4184 (2000).
[4]X. Zhang and Z. Liu, Nature Mater. **7**, 435 (2008).
[5]W. Cai, U. K. Chettiar, A. V. Kildishev, and V. M. Shalaev, Nat. Photonics **1**, 224 (2007).
[6]N. I. Landy, S. Sajuyigbe, J. J. Mock, D. R. Smith, and W. J. Padilla, Phys. Rev. Lett. **100**, 207402 (2008).
[7]W. Withayachumnankul, H. Lin, K. Serita, C. M. Shah, S. Sriram, M. Bhaskaran, M. Tonouchi, C. Fumeaux, and D. Abbott, Opt. Express **20**, 3345 (2012).
[8]W. Withayachumnankul, K. Jaruwongrungsee, A. Tuantranont, C. Fumeaux, and D. Abbott, Sens. Actuators, A **189**, 233 (2013).
[9]T. Driscoll, G. O. Andreev, D. N. Basov, S. Palit, S. Y. Cho, N. M. Jokerst, and D. R. Smith, Appl. Phys. Lett. **91**, 062511 (2007).
[10]Y. Sun, X. Xia, H. Feng, H. Yang, C. Gu, and L. Wang, Appl. Phys. Lett. **92**, 221101 (2008).
[11]H. T. Chen, J. F. O'Hara, A. K. Azad, A. J. Taylor, R. D. Averitt, D. B. Shrekenhamer, and W. J. Padilla, Nat. Photonics **2**, 295 (2008).
[12]A. E. Nikolaenko, N. Papasimakis, A. Chipouline, F. D. Angelis, E. D. Fabrizio, and N. I. Zheludev, Opt. Express **20**, 6068 (2012).
[13]A. K. Azad, H. T. Chen, X. Lu, J. Gu, N. R. Weisse-Bernstein, E. Akhadov, A. J. Taylor, W. Zhang, and J. F. O'Hara, Terahertz Sci. Technol. **2**, 15 (2009), available at http://www.tstnetwork.org/March2009/tst-v2n1-15Flexible.pdf.
[14]M. Walther, A. Ortner, H. Meier, U. Loffelmann, P. J. Smith, and J. G. Korvink, Appl. Phys. Lett. **95**, 251107 (2009).
[15]N. R. Han, Z. C. Chen, C. S. Lim, B. Ng, and M. H. Hong, Opt. Express **19**, 6990 (2011).
[16]Z. C. Chen, N. R. Han, Z. Y. Pan, Y. D. Gong, T. C. Chong, and M. H.Hong, Opt. Mater. Express **1**, 151 (2011).
[17]I. E. Khodasevych, C. M. Shah, S. Sriram, M. Bhaskaran, W. Withayachumnankul, B. S. Y. Ung, H. Lin, W. S. T. Rowe, D. Abbott, and A. Mitchell, Appl. Phys. Lett. **100**, 061101 (2012).
[18]H. Tao, A. C. Strikwerda, K. Fan, C. M. Bingham, W. J. Padilla, X. Zhang, and R. D. Averitt, J. Phys. D: Appl. Phys. **41**, 232004 (2008).
[19]Z. Chen, R. Mohsen, Y. Gong, T. C. Chong, and M. Hong, Adv. Mater. **24**, OP143 (2012).
[20]S. Lee, S. Kim, T. T. Kim, Y. Kim, M. Choi, S. H. Lee, J. Y. Kim, and B. Min, Adv. Mater. **24**, 3491 (2012).
[21]T. Sakurai, and K. Tamaru, IEEE Trans. Electron Devices **30**, 183 (1983).
[22]M. Choi, S. H. Lee, and Y. Kim, Nature **470**, 369 (2011).
[23]E. Pettenpaul, H. Kapusta, A. Weisgerber, H. Mampe, J. Luginsland, and I. Wolff, IEEE Trans. Microwave Theory Tech. **36**, 294 (1988).
[24]I. J. Bahl, *Lumped Elements for RF and Microwave Circuits* (Artech House Microwave Library, Boston, 2003), pp. 229–252.
[25]I. A. I. Al-Naib, C. Jansen, N. Born, and M. Koch, Appl. Phys. Lett. **98**, 091107 (2011).
[26]C. M. Shah, S. Sriram, M. Bhaskaran, M. Nasabi, T. G. Nguyen, W. S. T. Rowe, and A. Mitchell, J. Microelectromech. Syst. **21**, 1410 (2012).
[27]J. C. Lötters, W. Olthuis, P. H. Veltink, and P. Bergveld, J. Micromech. Microeng. **7**, 145 (1997).
[28]S. P. Lacour, D. Chan, S. Wagner, T. Li, and Z. Suo, Appl. Phys. Lett. **88**, 204103 (2006).